Integration and alignment through mechanical measurements: the example of the ESPRESSO front-end units

Matteo Aliverti[*a,b], Giorgio Pariani[a], Manuele Moschetti[a,b], Marco Riva[a]
[a]Osservatorio Astronomico di Brera, Via Emilio Bianchi 46, Merat, Italy; [b]Politecnico di Milano, Piazza Leonardo da Vinci 32, Milano, Italy

ABSTRACT

Traditional techniques usually rely on optical feedback to align optical elements over all the degrees of freedom needed. This strongly iterative process implies the use of bulky and/or flexible adjustable mountings.

Another solution under study consists in the characterization of every optomechanical elements and the integration of the parts without any optical feedback. The characterization can be performed using different 3D Coordinate Measuring Machines (like Laser Tracker, Articulated Arms and Cartesian ones) and referencing different parts like the optomechanical mounts or the optical surfaces. The alignment of the system is done adjusting the six degrees of freedom of every element with metallic shims. Those calibrated elements are used to correct the interfaces position of the semi-kinematic system composed by 3 screws and 3 pins.

In this paper, the integration and alignment of the ESPRESSO Front End Units (FEUs) will be used as pathfinder to test different alignment methods and evaluate their performances.

Keywords: ESPRESSO, Front End, Faro Arm, Coordinate Measuring Machine, Alignment, Integration

1. INTRODUCTION

High-resolution spectrographs play an important role in astrophysics and in the last 2 decades a number of those instruments have been designed and used to search for extra-solar planets using the Radial Velocity (RV) method.

The state of the art for RV measurements as of 2016 is the High Accuracy Radial velocity Planet Searcher (HARPS), an instrument installed in 2003 at the 3.6 m telescope in La Silla (Chile). It has a resolving power of 110000 and a long term RV accuracy of about 1 m/s making the discovery of hundreds of exoplanets possible.

After years of operation of this instrument (and its twin, HARPS-N), lots of RV uncertainty sources have been identified [1]. Those sources can be intrinsic in the observation or due to the design of the telescope and the instrument. More in detail, the 5 main factors are: stellar oscillation noise, stellar activity-related jitter, photon noise, ThAr calibration source and guiding noise.

This knowledge, together with the scientific driver of searching for earth like exoplanets, pushed for a new ultra-high resolution spectrograph: ESPRESSO (Echelle Spectrograph for Rocky Exoplanets and Stable Spectroscopic Observations).

1.1 ESPRESSO

The ESPRESSO spectrograph will be installed in Paranal in 2017 and will collect the incoherent light from 1 to 4 UTs (Unit Telescopes) of VLT (Very Large Telescope) [2] and will be fed by the Coudé Train (CT) and the Front End (FE).

The CT is composed by 4 prisms, 2 mirrors and 2 lenses for each UT and should bring their light to a convergence point located into the Combined Coudé Lab (CCL) [3].

[*] matteo.aliverti@brera.inaf.it; phone +393471504637

Ground-based and Airborne Instrumentation for Astronomy VI, edited by Christopher J. Evans, Luc Simard, Hideki Takami
Proc. of SPIE Vol. 9908, 99087C · © 2016 SPIE · CCC code: 0277-786X/16/$18 · doi: 10.1117/12.2233998

The FE is built around the convergence point and should inject the light coming from the CT or the Calibration sources into 6 scientific fibres depending on the observation mode chosen [4].

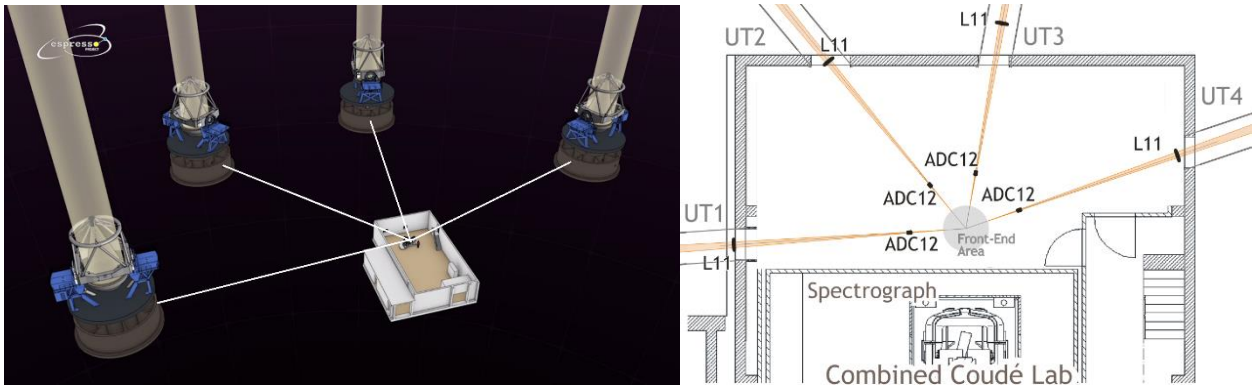

Figure 1. Left: view of the 4 UTs and the CCL where the ESPRESSO spectrograph will be installed. Right: CCL detailed view where the positions of the Front End and of the Spectrograph are shown.

The expected RV accuracy of the instrument is about 10 cm/s on quiet solar-type stars and must be stable for long periods. This value will be obtained using different techniques from the technological point of view: fibre scrambling, field and pupil stabilization for the fibre injection and overall mechanical stability of the system.

To guarantee this stability all the elements have been fixed in a semi-kinematic manner using 3 screws and 3 pins and, therefore, must have been aligned with the minimum number of iterations.

2. FRONT END OPTOMECHANICAL DESIGN

The FE is shown in Figure 2 and is composed by 4 equal FE Units (FEUs) used to inject the light beam coming from the star, the sky or the calibration source into the fibres and one toggling for the selection of different operative modes: Ultra High Resolution and High Resolution mode with the light of one of the 4 UTs, or Normal Resolution mode with the light of 1, 2, 3 or 4 UTs together. Before each FEU there's also an Atmospheric Dispersion Corrector composed by 2 counterrotating prisms. More details can be found in [4].

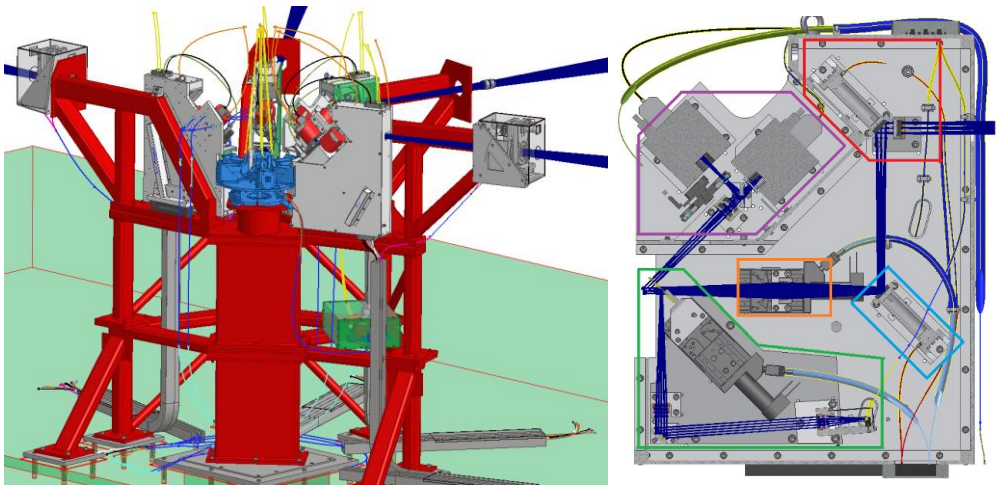

Figure 2. Left: overall view of the FE with the FE structure (red), the toggling system (light blue) and the FEUs (gray). Right: detailed view of one FEU. The light goes from top right to centre left.

The design of the optomechanical and mechanical elements of the system together with the developed alignment strategies have been done to obtain:

- High stiffness and eigenfrequencies and long term stability for high RV accuracy
- High reproducibility to decrease repair time in case of stages or platform failures
- Accurate alignment of the elements for the best optical quality
- Compact optomechanical mounts and alignment features for a more packed system
- Well known optical axis with respect to mechanical interfaces.

2.1 FEU optical and mechanical design

The main path of each FEU is included between 2 focal planes: the entrance one is an F/22.8 beam is located at 554 mm from the convergence point of the CCL while the exit is an F/12.7 at 200 mm from the convergence point.

Near the first focal plane and after a field lens, a PiMicos S330 Piezo tiptilt is used to stabilize the pupil (both in the red box in Figure 2) followed by an identical tiptilt element located at the pupil plane and used to stabilize the field (light blue box). To correctly inject the light into the 2 fibres of the Fibre Link (target and sky) at the exit of the FEU a refocuser doublet is mounted over a PiMicos LS65 linear stage (orange box).

In the green box the calibration system is shown: the light coming from 2 calibration fibres are reinjected into the 2 target/sky scientific ones. The core of this subsystem is the PiMicos LS65 linear stage with a holed mirror mounted on it; this element permit simultaneous calibration with 4 different modes: target/sky, CalibA/sky, target/CalibB and CalibA/CalibB.

The purple box contains the guiding subsystem. After 2 doublets, 1 dichroic and a PiMicos AFW65 filter wheel there are 2 AVT BigEye g132b CCD cameras conjugated to the pupil and the field planes. The images obtained by those cameras are then used to correctly inject the beam via the 2 piezo tiptilt.

2.2 Semi-kinematic and kinematic mounts

As already anticipated every optomechanical element is mounted on the FEU bench with 3 screws and 3 pins in a semi-kinematic way (see Figure 3 on the left). Moreover, to allow interchangeability of the 5 FEUs (for the 4 UTs + 1 spare), to guarantee a short repair time and to avoid deformations of the FEUs themselves a fully kinematic mount is used to integrate them on the FE structure (a cross section is shown in the central image of Figure 3).

Two mirrored plates with a conic hole and a V groove are mounted on the bottom of each FEU and on the top of FE structure. Three and 2 degrees of freedom are fixed by placing a sphere into the conic holes, and a cylinder in the V grooves. This solution allows for a fast and repeatable mounting of the units.

The last degree of freedom is fixed with a screw and 2 spherical washers on the top of the FEU.

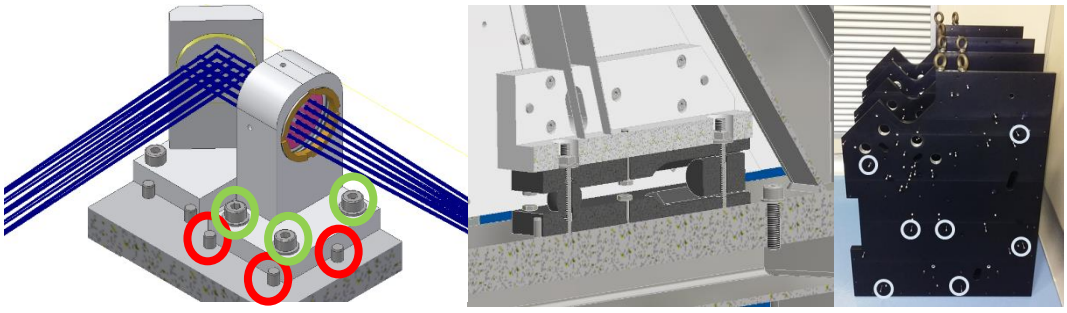

Figure 3. Left: two optomechanical elements with the semi-kinematic system. Centre: cross section of the kinematic bottom part. Right: the bench with in the light blue circles the 7 pins used as a reference for the kinematic mounts alignment.

3. ALIGNMENT PROCEDURE

The FEU alignment consisted in 3 main parts:

- Alignment of the FEU kinematic system on the bench
- Creation of a dummy FE structure and alignment of the performance evaluation system used to check the results (described in chapter 4. VERIFICATION METHODS AND RESULTS)
- Alignment of the optomechanical elements on the bench

3.1 FEU kinematic mounts alignment

The alignment of the bottom kinematic mounts has been done measuring the sphere and the cylinder once fixed into the upper grooves. The measurements have been performed with the Faro Arm EDGE an Articulated Arm Coordinate Measuring Machine (AACMM) with a Maximum Permissible Error (MPR) of 41 μm as of ASME B89.4.22-2004. In house tests also shown a repeatability of the machine below 10 μm when looking at one coordinate of a single point.

The first 3 degrees of freedom have been aligned with holed steel spacer below the screws then the remaining 3 degrees of freedom have been aligned with 3 pulling screws. Once all the degrees of freedom where aligned the kinematic mount screw have been tightened.

In order to define a common reference system between the benches, 7 pins have been chosen for the alignment. More in detail the reference system derived by the best fit between the nominal and the actual intersection of the axis of each pin into the bench plane.

In Table 1 the results obtained are shown. During the alignment, the nominal values have been continuously updated to minimize the peek to valley error.

Once all the kinematic mounts have been aligned on the bench side, a dummy FE structure has been built onto an optical table. All the FEUs benches have then been sequentially mounted on it for the optomechanical components alignment. A common reference system related to the dummy FE structure itself has been defined in order to avoid the uncertainties due to the Kinematic mounts alignment.

Table 1. Maximum deviation from the corrected nominal values of sphere and cylinder positions

[μm]	**Sphere**			**Cylinder**	
	X	**Y**	**Z**	**Y**	**Z**
UT0	-28	-16	+16	**-49**	**+44**
UT1	**-33**	-17	**+39**	+45	+23
UT2	+6	**-20**	+44	+10	+14
UT3	+28	**+20**	-37	+12	-38
UT4	**+33**	+9	**-44**	**+49**	**-44**
P-V	**66**	**40**	**88**	**98**	**89**

3.2 Optomechanical elements alignment procedure

For a proper alignment of the optical elements three different procedures have been tested.

The **first** method relied onto the tight tolerances of the optomechanical mounts and consisted in placing all the pieces in FE bench in their nominal position measuring the interfaces between each element and the FEU pins with the Faro Arm EDGE. Observing the results with the alignment verification system error bigger than expected have been found.

The correction of the refocused lenses position and tiptilt, done to respectively re-centre the field and the pupil in the Fibre Link focal plane, has been performed without success: all the elements where placed strongly out-of-axis and, as a consequence, the image quality was reduced.

This result can be justified considering the large number of uncontrolled uncertainty sources and a presence of systematic errors due to the milling machine used (later measurements of the mechanical elements showed in-tolerance perpendicularity errors of the interfaces planes, producing a tilt of all the elements always in the same direction).

The **second** method will not be presented in detail here, but it consists in the characterization of the beam of an interferometer followed by the alignment of each optical element and its mounting. At the end of this process 6 points have been acquired with the Faro Arm EDGE and used to align the element in the 6 degrees of freedom.

This method shown a lack of accuracy due to the low stiffness of the 5 degrees of freedom alignment system and the large number of sequential measurements required. If those problems can be overcome with stiffer alignment system and more accurate measuring machines, 2 other problems remain.

First of all, for refractive elements there is an ambiguity between tiptilt and decentre. The 'minimum coma zone' can be found spanning between all the possible combinations but with a low accuracy and performing an extremely time consuming procedure. The second problem is again related to the time needed for the aliment process also for reflective elements.

Due to those problems this method has only been used in the final alignment process to characterize the CMOS sensor of the camera used for the alignment verification (see chapter 4. VERIFICATION METHODS AND RESULTS).

The **third** method consists in the characterization of each mechanical mounting with a Coord3 Universal Coordinate Measuring Machine (CMM). This machine has a MPE of 1.8+L/333 μm as of ISO 10360-2:2009 and has been used to define 6 reference points for the 6 degrees of freedom of each element with respect to the cylindrical hole roughly determining the optical axis (see central image in Figure 4).

After gluing all the optics inside the mounts, the 6 reference points have been used to position the optomechanical element into the bench and align them using calibrate steel shims. At the endo of the alignment, minimal adjustments have been done on the refocusing lens to re-centre the beam without affecting the optical quality of the system.

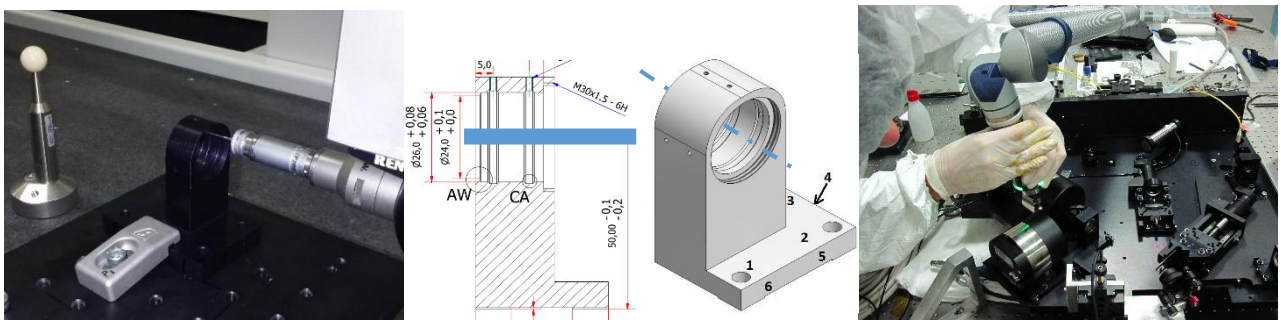

Figure 4. Left: the CMM during the characterization procedure of a lens mounting. Centre: a schematic representation of the optical axis and the 6 reference points. Right the alignment of the elements onto a FEU bench with the AACMM

This method has been used for the final alignment of the FEUs as it was characterized by high predictability of the results together with a quite fast characterization and alignment procedure.

4. VERIFICATION METHODS AND RESULTS

In order to verify if the alignment strategy was feasible and reliable a telescope simulator has been designed and aligned with respect to the dummy FE structure. Into the telescope simulator 2 mask have been used to check the pupil and the field quality.

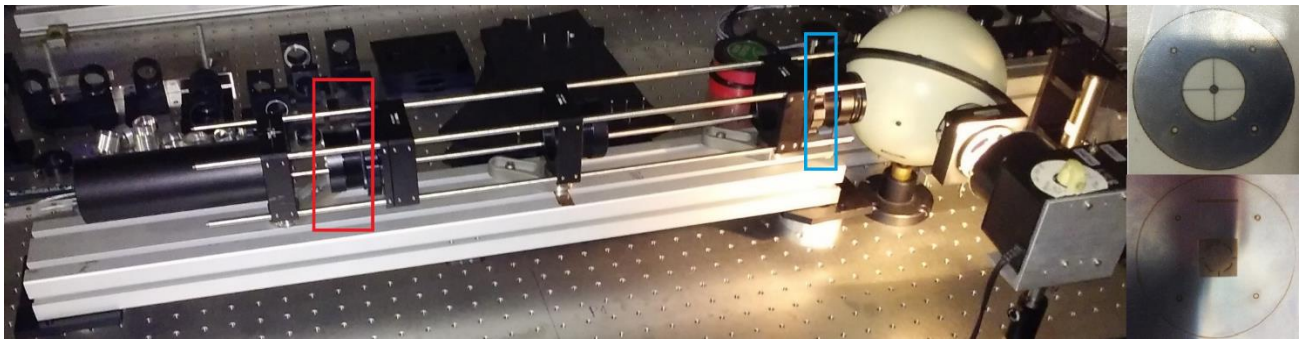

Figure 5. The Telescope Simulator with the pupil mask (shown at top right and marked with a red square) and the field mask (shown at bottom right and marked with a light blue square)

To verify the field optical quality a Thorlabs DCC1545M CMOS camera has been characterized with the second method previously described (see chapter 3.2) and placed at the Fibre Link focal plane. The pattern drawn into the field mask (a hole's matrix spaced of 250 μm each one with a diameter of ~25 μm) is imaged into that plane to verify the main path alignment quality. The alternate insertion of a 22.5° mirror instead of the CMOS sensor is then used to see the pattern onto the AVT Bigeye CCD field camera to evaluate the guiding path alignment quality (see Figure 6).

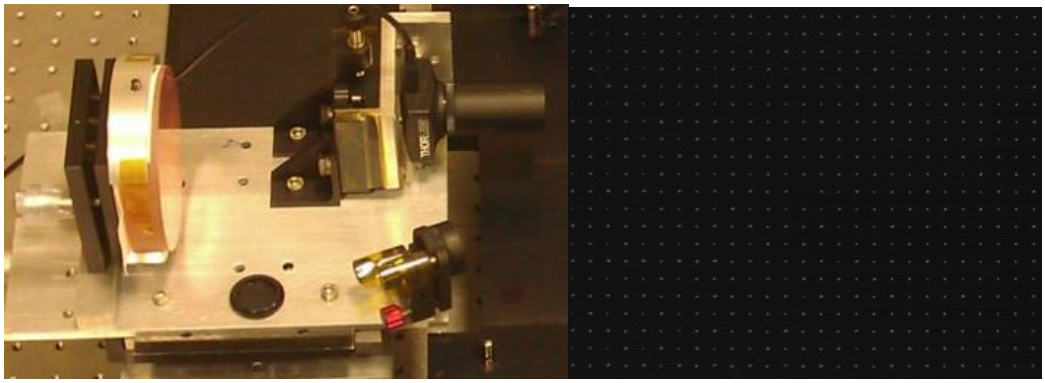

Figure 6. Left: the xy linear stage with the CMOS camera used to check the field quality, the 22.5° mirror and the perpendicular mirror for the pupil check. Right: hole's matrix as seen by the CMOS camera; note the missing hole at the centre of the mask.

The quality of the pupil through the main path has been evaluated placing a mirror (see Figure 6) on the exit focal plane, covering half of the pupil mask and checking the return of the non-covered half pupil back onto the paper used to cover the other half. Again, for the check of the guiding path the insertion of the 22.5° mirror has been used to see the pupil onto the AVT Bigeye pupil camera.

4.1 Online and final alignment verification

The optical quality has been verified during the alignment acquiring images and calculating, with a Matlab script, the decentring of the field and the Full Width at Half Maximum (FWHM) of all the holes (see Figure **7**). Small alignment

corrections have been performed in case the quality was not considered sufficient or the stroke of the tiptilt used to correct field and pupil exceeded the 5%.

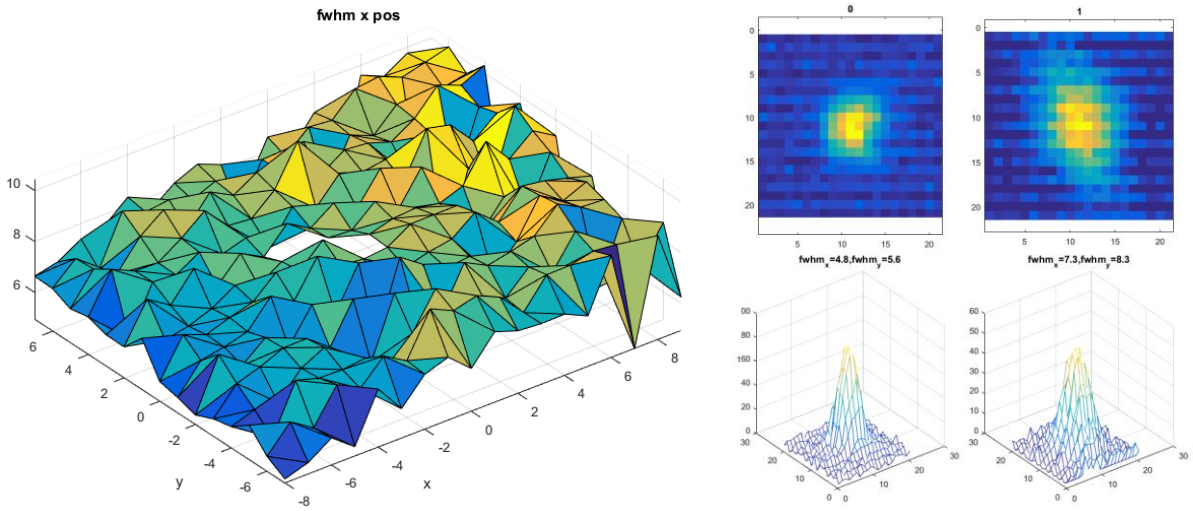

Figure 7. Example of FWHM calculation. It is possible to notice a tilt related error of the main path

At the end of the alignment process the images of the field, obtained from the CMOS and the CCD camera, have been evaluated in a more rigorous way (background subtraction, deconvolution to evaluate the Point Spread Function of the system and best fit with a Gaussian model). With the obtained model the Encircled Energy in a radius of 0.09 arcsec has been evaluated and is shown in Table 2 in both fibre link injection plane and guiding filed camera.

The results at the fibre injection plane level are quite constant and well above the requirements, while the guiding camera values are way more dispersed due to the presence of 2 collimation-refocusing doublets, impossible to align one relatively to the other.

Table 2. Encircled Energy values (%) for the 4 FEUs

UT	Fibre Link Injection					TCCD guiding field camera				
	TL	TR	BL	BR	CENTRE	TL	TR	BL	BR	CENTRE
1	91	93	92	91	**94**	97	92	95	91	**95**
2	93	93	94	90	**97**	89	65	93	78	**95**
3	96	94	95	92	**95**	97	76	97	80	**96**
4	90	96	90	95	**95**	93	80	91	88	**83**
REQ	80	80	80	80	**80**	-	-	-	-	-

4.2 Expected results and limitations of the method

During the alignment a Matlab script has been developed in order to predict the decentring error of the optical axis at the Fibre Link Injection level. Its output is shown in Figure 8.

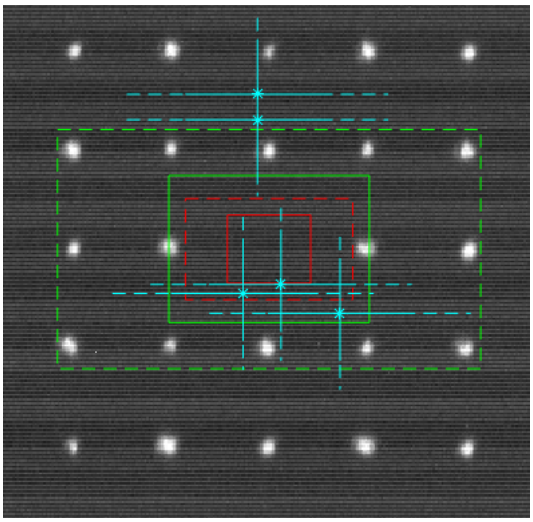

Figure 8. Expected decentring at the Fibre Link injection for the 5 FEUs

The green rectangles delimit the area where the centre of the optical axis should fall considering the uncertainty of the AACMM as the MPE stated by the manufacturer and the possible misalignments between the optical axis and the axis of the cylinder of each mechanical mounts.

Those misalignments have been calculated considering the geometrical characteristics of the optical and mechanical elements like cilindricity tolerances of the relative interfaces, diameter differences and length of the lenses.

All those values have been passed through the sensitivity analysis matrix of the system to calculate the full lines rectangle with a statistical approach and the dashed lines one with a worst case approach.

The light blue points represent the 5 FEUs expected position considering the remaining misalignment errors over the 6 degrees of freedom due to the imperfect alignment with the calibrated steel shims.

Another way to look at the image is considering the red rectangles where the size is calculated only considering the misalignment/play between the axis and the light blue band representing the uncertainty of the AACMM.

The meaning of the full/dashed lines remains the same as before.

The light blue points obtained from this simulation are compatible with the centres positions seen with the CMOS camera (data not shown here) proving that the script is reliable and can be used to check the expected results.

A few considerations can be also done considering the data from the script and the experience acquired:

- The use of this script during the alignment could have shown possible improvements of the alignments itself for 2 of 5 benches even before an image is available at the Fibre Link plane
- The use of a Cartesian CMM instead of the AACMM could reduce the length of the blue lines of almost two order of magnitude
- Even with a perfect measurement system the repeatability of the semi-kinematic mounts must be increased to allow for a faster and more accurate alignment (light blue dots moving to the centre of the image)
- The Worst Case approach better match the real system. This is related to bias in both the AACMM measurements and the lens-optomechanical elements mounts (e.g. all the elements tilted of decentred in the same direction during the gluing procedure)
- The red rectangles shown the intrinsic limits of this method. Even with a ‘perfect’ measuring machine and a perfect alignment there will be a certain amount of uncertainty due to the play between optical and mechanical elements.

5. CONCLUSIONS

The different methods tested for the successful alignment of the FEUs have been described. The Front End has passed the preliminary acceptance at INAF Merate and it's ready for the final acceptance in Genève. The study performed over the FEUs showed that it's possible to align an optical system with only mechanical references and predict with a good accuracy it's optical behaviour. A number of limitations have been found with the described methods and studies are ongoing to overcome them, together with improvements in terms of accuracy and reproducibility.

REFERENCES

[1] Lovis C, Pepe F, Bouchy F, Curto GL, Mayor M, Pasquini L, Queloz D, Rupprecht G, Udry S, Zucker S. The exoplanet hunter HARPS: unequalled accuracy and perspectives toward 1 cm s-1 precision. In SPIE Astronomical Telescopes+ Instrumentation 2006 Jun 14 (pp. 62690P-62690P). International Society for Optics and Photonics.

[2] Mégevand D, Zerbi FM, Di Marcantonio P, Cabral A, Riva M, Abreu M, Pepe F, Cristiani S, Lopez RR, Santos NC, Dekker H. ESPRESSO: the radial velocity machine for the VLT. In SPIE Astronomical Telescopes+ Instrumentation 2014 Jul 8 (pp. 91471H-91471H). International Society for Optics and Photonics.

[3] Cabral A, Abreu M, Coelho J, Gomes R, Monteiro M, Oliveira A, Santos P, Ávila G, Delabre BA, Riva M, Di Marcantonio P. ESPRESSO Coudé-Train: complexities of a simultaneous optical feeding from the four VLT unit telescopes. InSPIE Astronomical Telescopes+ Instrumentation 2014 Jul 28 (pp. 91478Q-91478Q). International Society for Optics and Photonics.

[4] Riva M, Aliverti M, Moschetti M, Landoni M, Dell'Agostino S, Pepe F, Mégevand D, Zerbi FM, Cristiani S, Cabral A. ESPRESSO front end: modular opto-mechanical integration for astronomical instrumentation. InSPIE Astronomical Telescopes+ Instrumentation 2014 Aug 6 (pp. 91477G- 91477G). International Society for Optics and Photonics